

UPDATE ON GRAVITATIONAL-WAVE RESEARCH *

L. P. Grishchuk

*Department of Physics and Astronomy, Cardiff University, Cardiff CF24 3YB, United Kingdom
and Sternberg Astronomical Institute, Moscow University, Moscow 119899, Russia*

E-mail: grishchuk@astro.cf.ac.uk

The recently assembled laser-beam detectors of gravitational waves are approaching the planned level of sensitivity. In the coming 1 - 2 years, we may be observing the rare but powerful events of inspiral and merger of binary stellar-mass black holes. More likely, we will have to wait for a few years longer, until the advanced detectors become operational. Their sensitivity will be sufficient to meet the most cautious evaluations of the strength and event rates of astrophysical sources of gravitational waves. The experimental and theoretical work related to the space-based laser-beam detectors is also actively pursued. The current gravitational wave research is broad and interesting. Experimental innovations, source modelling, methods of data analysis, theoretical issues of principle are being studied and developed at the same time. The race for direct detection of relatively high-frequency waves is accompanied by vigorous efforts to discover the very low-frequency relic gravitational waves through the measurements of the cosmic microwave background radiation. In this update, we will touch upon each of these directions of research, including the recent data from the Wilkinson Microwave Anisotropy Probe (WMAP).

I. INTRODUCTION

The concept of gravitational radiation has been with us for quite a long time. Thinking of the relativistic gravitational field in parallel with the familiar case of the electromagnetic field, it was natural to expect that there should exist waves of the gravitational field similar to the waves of the electromagnetic field. As Einstein [1] put it in 1913: “The conviction had to come that Newton’s law of gravitation is as incapable of describing all gravitational phenomena as Coulomb’s laws of electrostatics and magnetostatics are of electromagnetic phenomena”. The decades of hard work have followed. In the beginning, the research was purely theoretical. Through doubts and controversies, the conceptual and mathematical issues of gravitational radiation have been clarified. Then, in the 60-s, the experimental work has started with the pioneering effort of J. Weber [2]. In the 90-s, gravitational waves have been observed indirectly via the measurement of secular changes in the orbital parameters of the binary system of neutron stars that includes the pulsar PSR 1913+16 [3]. These days, gravitational waves are routinely taken into account in the theoretical and observational studies ranging from orbital evolution of close pairs of compact stars to the early Universe cosmology. The experimental progress has also been very impressive.

We are now at a special and decisive point. First, the relevance and importance of gravitational-wave research is fully recognised by the communities of physicists and astronomers. The worldwide network of scientific collaborations has been established, reflecting the necessity of coincident observations at various instruments and the need for joint analysis of the data [4], [5]. Second, the scientific runs have begun at the recently assembled sensitive laser-interferometric observatories - American LIGO [6] and British-German GEO600 [7]. The French-Italian VIRGO [8] will be operational soon. Meanwhile, the Japanese TAMA300 [9], along with the international network of bar detectors [10], continue to collect data at their level of sensitivity. The design sensitivity of three LIGO interferometers plus VIRGO and GEO600 meets the realistic astrophysical predictions, so the direct detection of powerful (even if rare) sources, such as coalescing stellar-mass black holes, becomes likely. Third, the European Space Agency (ESA) and American NASA have agreed to share the costs of the space-based Laser Interferometer Space Antenna (LISA) [11]. LISA is planned to be launched around the year 2011, preceded by a technology demonstration mission. The plans for the advanced ground-based detectors, such as LIGO II, the Japanese cryogenic laser interferometer LCGT, and, possibly, the European EURO, are also maturing very quickly. These instruments of the next generation will detect a host of well anticipated sources, such as compact binary stars, but really fundamental discoveries are also expected. Fourth, there exists a strong competition on the side of purely astronomical means of indirect detection of gravitational waves. In fact, the anisotropy and polarisation measurements of the cosmic microwave background radiation (CMB) are likely to bring us decisive information on the fundamentally important relic gravitational waves much earlier than

*To be published in the first volume of the “Astrophysics Update”, ed. J.W.Mason (Springer-Praxis, 2004) pp. 281-310

it will be done by direct methods. By all counts, gravitational-wave research is now one of the most exciting and promising areas of physical science.

The weakness of gravity as a physical interaction is the strength of gravitational waves as a tool of scientific research. It is difficult to detect gravitational waves because they carry their energy practically without scattering and absorption. But this is exactly because of this difficulty that we have any chance to learn about what was happening at the beginning of the Universe, or in the depth of an exploding supernova, or in the vicinity of, what we think are, merging black holes. It is also likely that the differing properties of gravitational waves will be a discriminating signature of different fundamental physical theories and modified gravities.

In this review, we will start, in Sec. 2, with an elementary theory of gravitational waves. Then, in Sec. 3, we will discuss the current status of gravitational-wave experiments. In Sec. 4 we will focus on astrophysical sources of gravitational waves and the new physics that will be learned from their observation. Sec. 5 is devoted to gravitational waves and cosmology. In particular, some recent results from the WMAP will be discussed in the context of gravitational-wave research, including the “implications for inflation”. Finally, we briefly summarise this update in Sec. 6. The background material on the gravitational-wave research can be found in [12], [13], [14], and some of the previous reviews in [15], [16], [17], [18], [19].

II. ELEMENTARY THEORY OF GRAVITATIONAL WAVES

There are some similarities in the mathematical description of the gravitational field and the electromagnetic field. The electromagnetic field can be described by the components of the 4-vector potential A^μ . The quantities A^μ are functions of time and spatial coordinates x^α , $x^\alpha = (ct, x, y, z)$, and they obey the wave-like dynamical equations - the Maxwell equations. Other quantities, such as electric and magnetic components \mathbf{E} , \mathbf{H} , and the energy-momentum tensor of the electromagnetic field, are calculable from A^μ . The quantities A^μ allow the gauge freedom. This means that some seemingly different solutions of the field equations are in fact equivalent solutions in the sense of their physical manifestations. Analogously, the gravitational field can be described by 10 components of the 4×4 symmetric tensor $h^{\mu\nu}$ as functions of x^α . The quantities $h^{\mu\nu}$ obey the nonlinear wave-like dynamical equations - the Einstein equations. The energy-momentum tensor of the gravitational field $t^{\mu\nu}$ is calculable from the tensor $h^{\mu\nu}$. The quantities $h^{\mu\nu}$ allow the gauge freedom, so that some seemingly different solutions of the gravitational field equations describe in fact the physically equivalent configurations.

In contrast to the electromagnetic field, the gravitational field $h^{\mu\nu}$ is a nonlinear field. This means that a sum of two solutions of the field equations is not a new solution, and the gravitational field, along with matter fields, is a source for itself. However, in a number of situations one can neglect the nonlinearity of the gravitational field. In this approximation we come to the notion of weak gravitational fields and linearised gravitational waves.

Many properties of linearised gravitational waves resemble those of electromagnetic waves. Gravitational waves propagate with the velocity of light c and have two independent transvers polarization states. In its action on free masses, a gravitational wave (g.w.) exhibits some analogs of the electric and magnetic contributions of an electromagnetic wave (em.w.) acting on free electric charges. Gravitational wave field is dimensionless and its strength can be characterized by a dimensionless amplitude h . The amplitude h decreases in the course of propagation from a localized source in inverse proportion to the traveled distance: $h \propto 1/r$. Gravitational waves carry away from a radiating system its energy, angular momentum and linear momentum.

The linearised g.w. satisfy the wave equation

$$h^{\mu\nu,\alpha}{}_{,\alpha} + \eta^{\mu\nu} h^{\alpha\beta}{}_{,\alpha,\beta} - h^{\nu\alpha,\mu}{}_{,\alpha} - h^{\mu\alpha,\nu}{}_{,\alpha} = 0, \quad (1)$$

where the ordinary derivative is denoted by a comma and $\eta^{\mu\nu}$ is the metric tensor of the Minkowski space-time:

$$d\sigma^2 = \eta_{\mu\nu} dx^\mu dx^\nu = c^2 dt^2 - dx^2 - dy^2 - dz^2. \quad (2)$$

The first term in Eq. (1) is the familiar d'Alembert (wave) operator. A plane-wave solution to Eq. (1) is given by

$$h^{\mu\nu} = a^{\mu\nu} e^{ik_\alpha x^\alpha}, \quad (3)$$

where $k_\alpha k^\alpha = 0$, reflecting the fact that a g.w. propagates with the velocity of light. Because of this condition, the field equations (1) require the 10 components of the constant matrix $a^{\mu\nu}$ to satisfy 4 constraints: $a^{\mu\nu} k_\nu = 0$. Then, the quantities a^{00} and a^{0i} can be expressed in terms of 6 components of the matrix a^{ij} . This matrix itself includes the part \tilde{a}^{ij} satisfying the further 4 constraints: $\tilde{a}^{ij} k_j = 0$, $\tilde{a}^{ij} \eta_{ij} = 0$. These remaining 2 degrees of freedom (sometimes called the TT-components) fully determine the observational manifestations of the plane wave and its energy-momentum characteristics. Indeed, it is easy to show that the gravitational energy-momentum tensor

$$t_{\mu\nu} = \frac{c^4}{32\pi G} \left[h^{\alpha\beta}{}_{,\mu} h_{\alpha\beta,\nu} - \frac{1}{2} h_{,\mu} h_{,\nu} \right] \quad (4)$$

depends only on the TT-components of the field:

$$t_{\mu\nu} = \frac{c^4}{32\pi G} k_\mu k_\nu [2\tilde{a}^{ij}\tilde{a}_{ij}^*], \quad (5)$$

where we have dropped (as we normally do in the case of electromagnetic waves) the purely oscillatory terms.

How does a gravitational wave affect the free (i. e. not subject to any other forces or constraints) masses? In the case of an em.w., we could have noticed the displacement of a charged particle with respect to a neutral particle placed initially in the same point. In the case of a gravitational wave, there is no particles neutral to the gravitational interaction, so we need to study the relative displacement of particles separated initially. This brings us to the analysis of tidal effects of a gravitational wave, similar to the tidal effects of a Newtonian gravitational field. Let one of free masses define the origin of our coordinate system, $x_{(1)}^i = 0$, whereas the second mass is placed initially at $x_{(2)}^i = l^i$ and its (small) displacement caused by the gravitational wave is denoted by ξ^i . Then the equations of motion of the second mass are:

$$\frac{d^2 \xi^j}{dt^2} = \frac{1}{2} \omega^2 \tilde{a}_k^j l^k e^{i\omega t}. \quad (6)$$

These equations depend only on the TT-components of the wave.

For a wave propagating, say, in z -direction it is convenient to write the TT-components explicitly:

$$h_{xx} = -h_{yy} = h_+ \sin(\omega t - kz + \psi), \quad h_{xy} = h_\times \cos(\omega t - kz + \psi). \quad (7)$$

Then, the relevant solution to Eq. (6) reads

$$x = l_1 - \frac{1}{2} l_1 h_+ \sin(\omega t + \psi) - \frac{1}{2} l_2 h_\times \cos(\omega t + \psi), \quad y = l_2 - \frac{1}{2} l_1 h_\times \cos(\omega t + \psi) + \frac{1}{2} l_2 h_+ \sin(\omega t + \psi), \quad z = l_3. \quad (8)$$

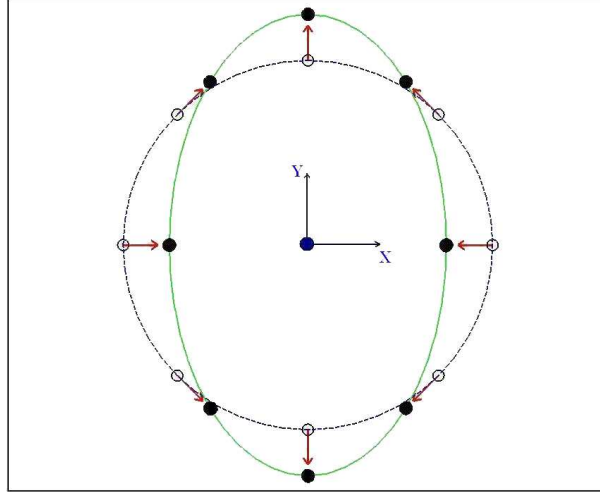


FIG. 1. Motion of free particles in the field of a linearly-polarised gravitational wave

The masses that lie (on average) on the ring $(l_1)^2 + (l_2)^2 = l^2, l_3 = 0$, oscillate around their ring positions. In Fig. 1 we show a quarter of the cycle caused by a wave with the $+$ polarization state (i.e. when $h_+ \neq 0, h_\times = 0$). The pattern of oscillations enforced by the \times polarization state (i.e. when $h_\times \neq 0, h_+ = 0$) can be obtained from Fig. 1 by its rotation by the angle 45° in the (x, y) plane. The general motion of a particle is a linear superposition of these oscillations, as seen in Eq. (8). The oscillatory deformation of a sphere of masses, surrounding the central mass at the origin, is described by a linear combination of spherical harmonics $Y_{lm}(\theta, \phi)$ with $l = 2$ and $m = \pm 2$, and where the polar axis is taken along the z direction.

Equations (8) suggest that the motion of free particles is confined strictly to the planes $z = const$. This conclusion comes about only because we have so far neglected the smaller terms, containing the products of h_+, h_\times with the extra

small factor l/λ , where l is the separation between masses and $\lambda = 2\pi c/\omega$ is the gravitational wavelength. When these terms are taken into account, the perturbed positions x, y and, most importantly, z receive further contributions. The gravitational wave drives the masses not only in the plane of the wave-front, but also, to a smaller extent, back and forth in the propagation direction [16]. This extra component of motion is similar to the one caused by the magnetic field and the Lorentz force of the em.w. acting on a charged particle. In Fig. 2 we show typical displacements of the masses forming (on average) the plane $z = 0$, when the “magnetic” contribution to their motion is also taken into account. It is seen from this figure that the entire plane of particles is being bent in an oscillatory fashion. This “magnetic” component of motion will play a certain role in the analysis of observations with laser interferometers [20].

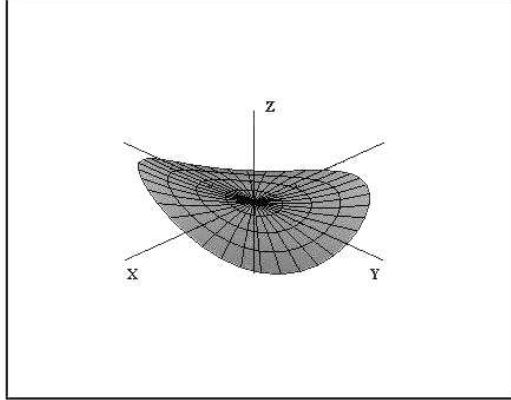


FIG. 2. Motion of free particles with the “magnetic” component taken into account

The amplitudes h_+, h_\times are determined by the source of the gravitational waves. To find the amplitudes, we should replace the zero in the right hand side of Eq. (1) by the source term $(16\pi G/c^4)T^{\mu\nu}$, where $T^{\mu\nu}$ is the energy-momentum tensor of the source, and seek the retarded solutions to the wave equation. Assuming that the distance R_0 to the source is much larger than the wavelength, one can write

$$h_+(k_\alpha) = \frac{1}{R_0} \frac{2G}{c^4} [\hat{T}^{11}(k_\alpha) - \hat{T}^{22}(k_\alpha)], \quad h_\times(k_\alpha) = \frac{1}{R_0} \frac{4G}{c^4} \hat{T}^{12}(k_\alpha), \quad (9)$$

where the Fourier components $\hat{T}^{\mu\nu}(k_\alpha)$ are defined by

$$\hat{T}^{\mu\nu}(k_\alpha) = \int \left(\int T^{\mu\nu}(t_r, r_0) d^3 r_0 \right) e^{-ik_\alpha x^\alpha} d^4 x$$

and t_r is retarded time. These formulas allow one to evaluate the typical amplitude h from a given source:

$$h \sim \frac{1}{R_0} \frac{GM}{c^2} \left(\frac{v}{c} \right)^2, \quad (10)$$

where M is the total mass of the source and v is the characteristic non-spherical velocity of the matter bulk motion. For a bound system like a binary star, $(v/c)^2 \sim GM/c^2 a$, where a is the size of the system. An accurate calculation for a binary in a circular orbit, consisting of masses M_1, M_2 separated by the distance a , and after averaging over the orbital period and orientation of the orbital plane, gives

$$h = (\langle h_+^2 \rangle + \langle h_\times^2 \rangle)^{1/2} = \left(\frac{32}{5} \right)^{1/2} \frac{1}{R_0} \frac{G^{5/3}}{c^4} \frac{M_1 M_2}{(M_1 + M_2)^{1/3}} (\pi f)^{2/3}, \quad (11)$$

where the emitted g.w. frequency f (in Hz) is

$$f = \frac{1}{\pi} \left[\frac{G(M_1 + M_2)}{a^3} \right]^{1/2}. \quad (12)$$

Note that the amplitude h depends on a particular combination of masses:

$$\frac{M_1 M_2}{(M_1 + M_2)^{1/3}} = \mathcal{M}^{5/3}, \quad \text{where } \mathcal{M} = \frac{(M_1 M_2)^{3/5}}{(M_1 + M_2)^{1/5}}, \quad (13)$$

so that $h \propto (1/R_0) \mathcal{M}^{5/3} f^{2/3}$ and \mathcal{M} is sometimes called a chirp mass.

III. CURRENT STATUS OF GRAVITATIONAL WAVE DETECTORS

The possible methods of detecting gravitational waves, as well as the associated difficulties, can be seen from the discussion above. Fig.1 is helpful for understanding the principles of mechanically coupled detectors (bar detectors) and electromagnetically coupled detectors (laser interferometers). A bar detector is essentially a mechanical oscillator consisting of two masses connected by a spring. As an illustration, one can think of two elastically connected masses lying, say, at the opposite ends of the x axis in Fig. 1. The size of bar detectors is normally small, a couple of meters or so. A bar detector is a relatively narrow-band instrument. It is mostly sensitive to g.w. frequencies in the vicinity of the main eigen-frequency of the bar. In the presently operating instruments the resonant frequency is around $\sim 1kHz$. There are some advantages in using spherically shaped mechanical detectors. The construction of such detectors is currently taking place (see, for example, [21]). While the operating bar detectors continue to collect useful information [22], [23], [24], we will concentrate on laser interferometers.

The laser interferometer technique is based on free masses-mirrors whose relative distances are monitored by bouncing light. A ground-based interferometer is normally an L -shaped configuration. The light beamsplitter is in the corner of L , while the reflecting mirrors are at the ends of the configuration and near the beam splitter. The central mass in Fig.1 is an illustration of the beamsplitter and corner mirrors, whereas the end mirrors are located, say, in the positive directions of x and y . Obviously, mirrors in real interferometers are not free masses, they are suspended like pendulums. But they behave essentially as free masses in their motion along the corresponding arm. The length of the arms of an interferometer can be large. For instance, it ranges from 600 meters in GEO600 to $4km$ in largest of LIGO interferometers. In contrast to bar detectors, laser interferometers are relatively broad-band instruments. They are sensitive to frequencies in the interval $\approx (30 - 10^4)Hz$. Fig.1 shows the simplest case of a single monochromatic wave with one polarisation state arriving from the orthogonal direction to the detector's plane, but the response of the detector to the general case of the incoming wave is also calculable.

It is clear from Eq. (8) that the relative displacement of free masses is proportional to the incoming wave amplitude h : $\delta l/l \approx h$. Which numerical values of h can be expected from astrophysical sources in the surrounding Universe? Consider one of the most powerful and efficient emitters - a pair of compact stars orbiting each other at a tight orbit. Specifically, consider two neutron stars with masses $M_1 = M_2 = 1.5M_\odot$ at the late stage of their inspiral. Orbiting each other at separation $a = 100km$, they emit gravitational waves at frequency $f = 200Hz$. The emitted intensity of radiation is very high by astronomical standards: $3 \times 10^{52}erg/sec$. Let the distance to the source be $R_0 = 100Mpc$. We cannot take this distance much shorter than $100Mpc$, because the expected number of such events per year in a smaller volume of the surrounding Universe would be less than 1. Then, formula (11) says that the amplitude at Earth is $h \approx 10^{-22}$. This is an incredibly small number. It enters any conceivable method of detection of gravitational waves and explains why it is so difficult to observe them. In a $4km$ long interferometer, we need to beat all the noises and measure the mirror's displacements at the level of $4 \times 10^{-17}cm$.

The interferometer monitors the time-dependent difference of the relative distance variations in the two arms. Using the terminology of solid state physics, this quantity is called the (dimensionless) strain. Regardless of the presence or absence of the useful g.w. signal, there will always be some strain noise $n(t)$ in the output of the detector. The mean-square value of the noise can be expressed as an integral over the noise power spectral density $S_n(f)$:

$$\overline{n^2(t)} = 2 \int_0^\infty S_n(f)df. \quad (14)$$

The square root of $S_n(f)$ is the noise amplitude $\sqrt{S_n(f)}$. This quantity has the dimensionality of $Hz^{-1/2}$, and it is this quantity that is usually plotted on the sensitivity graphs. In Fig. 3 (taken from [6]) we show the recent status of the noise amplitudes in the $4km$ interferometer of the LIGO Livingston site. One can see the great progress that has been made on the way of reaching the design goal of sensitivity, shown by the solid line. The lower frequency part of the sensitivity curve is dominated by seismic perturbations, the central part by thermal noise in mirror's suspensions, and the higher frequency part by the shot noise of the laser light. The advanced LIGO sensitivity curve will be lower than the solid line in Fig.3 by a factor of 10 across all the frequencies. This upgrade of LIGO is planned to take place in about the year 2007. The advanced instruments will also allow optical configurations in which the sensitivity can be increased in a certain narrow frequency band at the expense of lowering the sensitivity outside the chosen band.

To compare qualitatively the astrophysical signal S , represented by the dimensionless amplitude h , with the detector's r.m.s. noise N , we should calculate, as formula (14) suggests, the product $\sqrt{S_n(f)}\sqrt{\Delta f}$, where Δf is the appropriate bandwidth in the noise spectrum. Taking the initial LIGO design sensitivity $3 \times 10^{-23}Hz^{-1/2}$ at $f = 200Hz$ and $\Delta f = f$, we would get $\sqrt{S_n(f)}\sqrt{\Delta f} = N = 5 \times 10^{-22}$. This N is a factor of 5 higher than the signal $S = 10^{-22}$ from the coalescing neutron stars considered above. The ratio $S/N = 1/5$ would suggest that, by a significant margin, the signal is not measurable. The reality, however, is somewhat better than this estimate. One should take into account the a priori knowledge of the expected waveform. If the waveform is known, one can

use the well developed technique of matched filtering. This method recovers the signal by, effectively, reducing the appropriate Δf and the relevant amount of detector's noise. For a quasi-periodic signal, this is achieved by using a long observation time T : $1/T \sim \Delta f \ll f$. In the case of a coalescing binary, the dominant g.w. frequency is increasing with time, but the binary still executes almost $n = 200$ cycles before changing its frequency by a factor of 2. This points out to a possible increase of the estimated S/N by a factor \sqrt{n} . The importance of accurate modelling of the expected waveforms is well appreciated. Presently, this is an important challenge for theorists (see, for example, [25]).

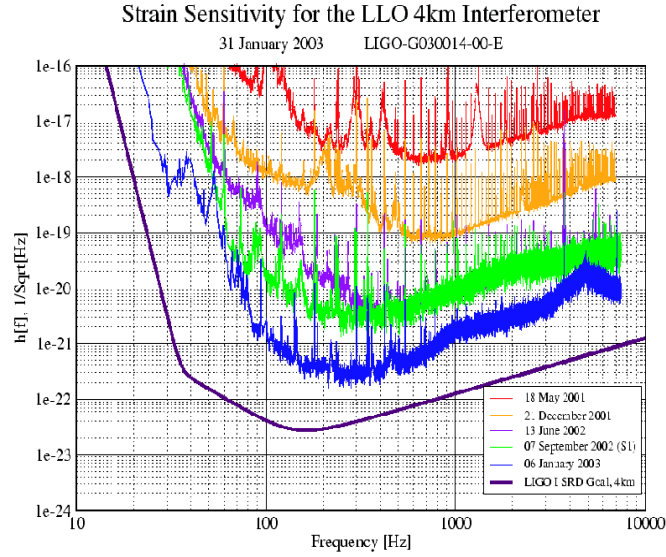


FIG. 3. The status of sensitivity of one of the LIGO interferometers

Fig. 4 (taken from [18]) shows the accurately calculated S/N ratios for the initial laser interferometers. As expected, the S/N grows with the total mass M of the coalescing binary, because the signal gets larger. However, binaries with the total mass greater than about $80M_{\odot}$ radiate at too low frequencies before merging. At these low frequencies the detector noise is high, as seen in Fig. 3. Therefore, the S/N decreases again. Certainly, the equal mass binaries with the total mass greater than $M \sim 10M_{\odot}$ can only be pairs of black holes, according to our present understanding of stars and stellar evolution.

The LIGO-GEO collaboration has reported [26] the first upper limits on coalescing binary systems, as well as other possible g.w. sources. These limits were derived from observations at the currently achieved sensitivity. They are not yet significant from the astrophysical point of view, but, outside the frequency interval probed by the bar detectors, they are tighter than other upper limits experimentally established so far. The necessary steps for increasing the sensitivity in the initial and advanced ground-based interferometers are well recognised and are being taken up.

The space-based interferometer LISA will be sensitive to g.w. in the interval $10^{-4} - 10^0 Hz$, that is, to lower g.w. frequencies as compared with ground-based instruments. Some new types of astronomical sources will be accessible to this detector. LISA will consist of three spacecraft, forming an equilateral triangle of side 5 million km, in a heliocentric orbit, lagging behind the Earth by 20° . The phase shifts of the laser light traveling along all three sides of the triangle will monitor the light-travel distance between the small drag-free test masses inside the spacecraft. The nominal lifetime of the mission is 5 years. Fig.5 shows the LISA design sensitivity curve and some of interesting sources of gravitational waves. This single figure attempts to show the noise curve of the entire assembly of spacecraft together with the strengths of g.w. sources of different nature - from quasi-periodic to stochastic - and therefore the figure should be treated with some care. The instrumental noise level is shown here in bins of $3 \times 10^{-8} Hz$, which are appropriate for a 1 year integration time. In other words, the r.m.s. instrumental noise $\sqrt{S_n(f)}$ in units of $(Hz)^{-1/2}$ (see Eq.(14)) is multiplied with $\sqrt{3 \times 10^{-8} Hz}$ at each frequency, thus producing a dimensionless spectral quantity. (For the latest amendments of the LISA noise curve see, for example, [27].) This is done mainly in order to emphasize that during this observational time the g.w. signals from many of the galactic white-dwarf binaries can be resolved and removed from the data. This means that their g.w. noise will not prevent us from seeing something much more interesting - a stochastic background of relic gravitational waves. The sharp drop of signal from the galactic binary

white dwarfs, shown in Fig.5 at $f = 2 \times 10^{-3} Hz$, illustrates this assumed operation with the data [18], [28], [29], and not the total lack of galactic binaries radiating at frequencies higher than $2 \times 10^{-3} Hz$. The continuation of this curve at $f > 2 \times 10^{-3} Hz$ shows the much smaller g.w. noise from unresolved extragalactic white dwarf binaries. In accord with this way of describing the dimensionless instrumental noise, the dimensionless g.w. signal amplitudes are also calculated in bins of $3 \times 10^{-8} Hz$ around any given frequency f . In the next section, we will present more details on astrophysical sources for ground-based and space-based instruments.

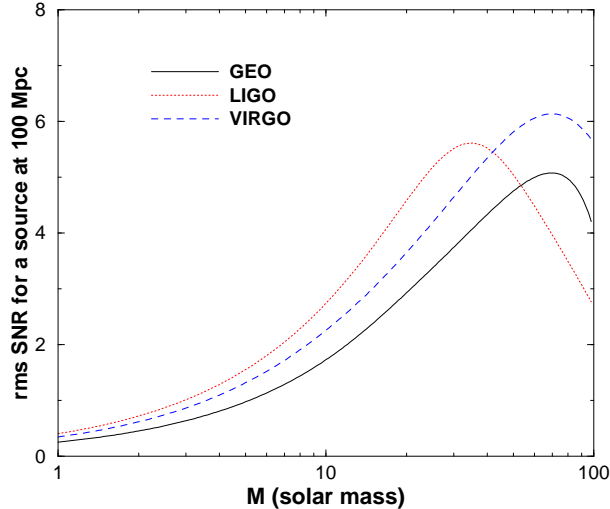


FIG. 4. Signal to noise ratio in initial interferometers as a function of total mass for inspiral signal from binaries of equal masses and averaged over source inclination

IV. GRAVITATIONAL WAVES AND ASTROPHYSICS

It is common to divide the sources in groups, depending on whether they are accessible to ground-based or space-based instruments. It is also common to call them, respectively, the high-frequency and low-frequency sources.

A. High-frequency sources

We will focus on the sources that are likely to be the first sources detected by the ground-based instruments. It is clear from Eq. (10) that a powerful source of gravitational waves should involve large masses and relativistic velocities. A pair of neutron stars inspiraling toward each other under the influence of the g.w. radiation reaction force is a primary example. In the last few seconds of inspiral, before the neutron stars “touch” each other and merge, the frequency of gravitational radiation increases from $200 Hz$ to about $1200 Hz$. The orbital velocity increases from $v/c \approx 0.2$ to $v/c \approx 0.4$. In the last few seconds the binary emits $1.1 \times 10^{53} ergs$ of energy in the form of gravitational waves. This is a 2% of its total rest-mass energy Mc^2 . What can be more powerful and efficient a source of gravitational radiation than this one? Only a pair of even more massive and even more compact stars. Astronomers call them stellar-mass black holes.

If the coalescence of a binary neutron star (NS+NS) or a binary black hole (BH+BH) happened in our Galaxy, it would be easily detectable by the already operating instruments. The problem is that these catastrophic events are expected to take place only once per a very long while. In order to have a reasonable chance of seeing, say, 3 events per year, we have to survey a large volume of space, which includes many galaxies. This means that the instrument’s sensitivity should be so high, that the events could be seen from the edges of this large volume. This consideration explains the importance of theoretical evaluations of the event rates in a typical galaxy.

The event rate of coalescing NS+NS systems is partially constrained by pulsar observations in our Galaxy. Three NS+NS binaries are known, each involving a pulsar, whose coalescence time is less than the Hubble time and is, on average, 3×10^8 years. Starting with these 3 binaries, one would evaluate the NS+NS event rate as 1 per 100 million years. However, we observe only about 1% of the galactic volume, so the coalescence rate can easily be raised to $10^{-6} yr^{-1}$ [30]. Very likely, the event rate for NS+NS systems is significantly higher than this estimate, if only because of the fact that not all NS+NS systems include a currently observable pulsar. The observational situation with black

holes is more uncertain. There are a dozen of BH candidates in X-ray binary systems, but they all are in pairs with non-degenerate companions. So far, there is no observational evidence for NS+BH or BH+BH binaries. Nevertheless, one can make some evaluations on the basis of the star formation rates.

It is believed that the neutron star progenitors have masses greater than $10M_\odot$, whereas the black hole progenitors have masses greater than $80M_\odot$. The Salpeter function for the star formation rate is

$$\frac{dN}{dt d(M/M_\odot)} \simeq \left(\frac{M}{M_\odot}\right)^{-2.35} yr^{-1}.$$

Integrating this function over M and using the lower limit of integration, one finds the ratio of the expected numbers of progenitors:

$$\frac{N(M > 80M_\odot)}{N(M > 10M_\odot)} = \left(\frac{80M_\odot}{10M_\odot}\right)^{-1.35} \simeq 0.06.$$

It is reasonable to think that, despite all the complexities and differences in binary evolution, the ratio of coalescence rates will also be given by approximately the same quantity,

$$\frac{\mathcal{R}_{BH}}{\mathcal{R}_{NS}} = \left(\frac{80M_\odot}{10M_\odot}\right)^{-1.35} \simeq 0.06.$$

This expectation turns out to be in rough agreement with the results of detailed numerical population synthesis calculations.

Numerical calculations take into account all the available observational information. Their advantage is in that one can follow not only the channels leading to the NS+NS, NS+BH, BH+BH systems, most interesting for gravitational-wave astronomy, but also other evolutionary outcomes, which allow comparison with observations in their own right. The population synthesis results cannot be less reliable than purely “observational” estimates, as they are controlled by the same available observational data. Discrepancies in final results exist because of uncertainties in astrophysics, not because one of the methods is inherently less reliable than another. This is especially true with regard to the NS+BH and BH+BH binaries, where the current purely “observational” evaluations would have to begin with zero.

The results of conservative population synthesis calculations [31], [18] have been checked on their consistency with other evolutionary outcomes. The calculations show that the NS+NS rate is expected to be at the level $\mathcal{R}_{NS} = 3 \times 10^{-5} yr^{-1}$, whereas the BH+BH rate is at least one order of magnitude lower. For further estimates we will take it at the level $\mathcal{R}_{BH} = 0.06 \mathcal{R}_{NS} = 2 \times 10^{-6} yr^{-1}$. These rates for a typical galaxy, \mathcal{R}_G , determine the rates for a given cosmological volume, \mathcal{R}_V , which includes many galaxies. When deriving the \mathcal{R}_V , it is convenient to use a conservative estimate for the baryon content of the Universe. This brings us to the relationship

$$\mathcal{R}_V \approx 0.1 \mathcal{R}_G \left(\frac{r}{1 \text{ Mpc}}\right)^3.$$

Thus, it is expected that within the volume of radius $r = 100 \text{ Mpc}$ and during 1 year, there will be 3 of NS+NS events and only 0.2 of NS+BH or BH+BH events. The increase of the radius to $r = 200 \text{ Mpc}$ increases the volume and the event rates by a factor 8. It is interesting to note that, despite all the diversity of approaches in the literature, there exists some tendency to convergence of the final results [32], [33], [34], [35], [36].

The derived event rates are the basis for the calculation of the expected detection rates. The important fact is that the mass of a typical neutron star is $1.4 M_\odot$, whereas the mass of a typical black hole is $(10 - 15) M_\odot$. The averaged mass of the observed black hole candidates in the X-ray binaries is $M_{BH} \simeq 8.5 M_\odot$. A pair of black holes is a more powerful source of gravitational waves than a pair of neutron stars, and therefore black hole binaries can be seen by a given instrument from much larger distances. When it comes to the detection rates, the lower event rate of BH+BH sources is more than compensated by their larger masses. Indeed, the optimal signal to noise ratio is [15], [37], [18]: $S/N \propto \mathcal{M}^{5/6}/r$. At a fixed S/N , the detection volume is proportional to r^3 and therefore to $\mathcal{M}^{5/2}$. The detection rate \mathcal{D} for binaries of a given class is the product of their event rate \mathcal{R}_V and the detector’s registration volume $\propto \mathcal{M}^{5/2}$ for these binaries. Therefore, one obtains

$$\frac{\mathcal{D}_{BH}}{\mathcal{D}_{NS}} = \frac{\mathcal{R}_{BH}}{\mathcal{R}_{NS}} \left(\frac{\mathcal{M}_{BH}}{\mathcal{M}_{NS}}\right)^{5/2} = 0.06 \left(\frac{8.5M_\odot}{1.4M_\odot}\right)^{5/2} \simeq 5.5.$$

This remarkable result is consistent with the more accurate numerical calculation of S/N displayed in Fig. 4.

It is seen from Fig.4 that g.w. signals from NS+NS at $r = 100Mpc$ cannot be regarded detectable by initial interferometers. The situation is much better for havier pairs of NS+BH and BH+BH. If the total mass of a BH+BH binary is near $(20 - 30)M_{\odot}$, then $S/N \approx 2$ even if the binary is placed at $r = 200Mpc$. It follows from the event rate \mathcal{R}_{BH} discussed above, that in this larger volume one expects a couple of BH+BH events per year. The simultaneous observations on two or three instruments will significantly diminish the probability of false alarms to such events. This is why it is argued in Ref. [18] that the coalescing black holes will probably be the first sources detected by the initial ground-based interferometers, when they reach their planned sensitivity. Of course, the discussed estimates are statistical by the very nature of things, and they have significant systematic unceratinties. It will not be very surprising if the reality is somewhat better or somewhat worse than what the mean values suggest. It is important, however, that even the most pessimistic evaluations of the NS+NS and BH+BH rates indicate that there should be many detections per year in the advanced interferometers.

If the coalescing black holes are detected first, it is likely that at the beginning we will only have a proof that the objects are black holes in astronomical sense - an inspiraling pair of heavy compact masses. The next step will be to try to understand their real physical nature. The general-relativistic black holes possess event horizons, which are supposed to merge into the resulting black hole, which will then emit a damped train of ringdown waves at specific frequencies, and so on [37], [38]. This fascinating physics will be testable when the good quality data are available. This analysis will also require the continuation of the intense effort on the side of analytical and numerical calculations (for a recent review of numerical relativity, see [39]).

Direct detection of first sources will be not the end, but only the beginning of the observational g.w. astronomy. In the long run, the aim of g.w. science is to explore a great variety of sources, many of which can hardly be seen in electromagnetic radiation. Needless to say that there is also a great chance of discovering new and totally unexpected sources. In addition to coalescing binary stars, many other sources will eventually be detected. For instance, the long-recognised importance of the core collapse of massive stars [40], [41] as g.w. sources has been reinforced by the mounting evidence of asymmetries during the supernova explosions, by the likelihood of forming and quick collapse of very massive early stars, by the association of supernovae events with gamma-ray bursts, etc. (For a recent review and extensive list of references, see for example [42].) The tidal disruption of a neutron star by its companion, the various sorts of stellar instabilities [43], the slightly deformed spinning neutron stars, young pulsars, and low-mass X-ray binaries [44], [45] - are also the astrophysically important and interesting g.w. sources that will be studied, very likely, by advanced detectors.

B. Low-frequency sources

It is common to call the low-frequency g.w. sources as “sources for LISA”. Some of them are displayed in Fig. 5. As explained in the previous section, the dashed line shows the g.w. confusion noise from the binary white dwarfs, WD+WD, mostly concentrated in the disk of our Galaxy. LISA will not only detect thousands of WD+WD systems radiating at $f > 2 \times 10^{-3}Hz$, but is capable of doing this so accurately that their contributions can be removed individually from the data. Some known binaries consisting of degenerate and normal stars will also be detectable. Their angular coordinates and distance can be measured with high precision [46]. In fact, the well identified galactic binaries serve as guaranteed sources for LISA, and they will help to test LISA’s performance.

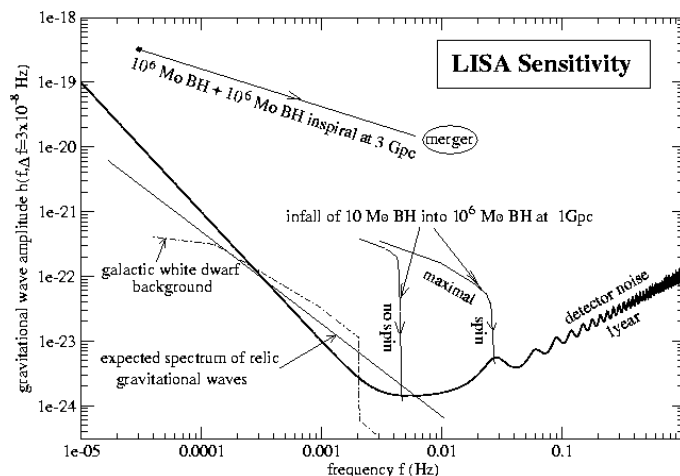


FIG. 5. Some interesting sources in comparison with LISA sensitivity

There is growing evidence for the existence of binary supermassive black holes (SMBH, $M \geq 10^6 M_\odot$) in the centers of merging galaxies. (For a recent review of SMBH formation see [47]). Certainly, a coalescing pair of SMBH is an extremely bright g.w. emitter. These sources are located at cosmological distances, so that the red shift of the incoming gravitational waves becomes important. But if the total mass of the pair is not significantly larger than $10^7 M_\odot$, the coalescing pair can still be visible by LISA at frequencies up to $f \approx 10^{-4} Hz$, even if the source is located at the red shift $z = 3$. The upper line in Fig.5 shows the effective gravitational wave amplitude, relative to the plotted LISA instrumental noise, for a source consisting of two SMBH. The dot shows the signal when the inspiraling pair was only 1 year prior to merger. The presence of spins of SMBH changes the LISA signal [48]. The trouble with these super-powerful sources is that their event rate is very uncertain. One of difficult issues is whether a SMBH forms by direct collapse of gas in deep galactic potential wells or by hierarchical build-up of pre-galactic structures. Nevertheless, it is estimated that LISA may see 0.1-1 events per year, or maybe a factor of 10 more [49].

It seems certain that, from time to time, a SMBH will be closely approached by nearby compact stars - white dwarfs, neutron stars and stellar-mass black holes. A compact star orbiting a SMBH is a powerful g.w. source. However its orbit and the emitted waveform depend strongly on the spin of SMBH. Fig.5 shows two curves (taken from [19]) describing the performance of a $10M_\odot$ BH completing its inspiral toward a $10^6 M_\odot$ SMBH. The left curve corresponds to a non-spinning SMBH and a circular orbit of a stellar-mass BH. The right curve describes the signal from a prograde, circular, equatorial orbit around a nearly maximally spinning Kerr SMBH. Both curves begin at frequencies when the time to merger is 1 year. A serious theoretical problem is the construction of reliable templates for these sources. One should expect that a typical orbit will be eccentric, non-equatorial, and subject to the radiation-reaction force corrections. Correspondingly, the waveforms could be extremely complicated. Some progress in this area is reported in [50].

Finally, Fig.5 shows the expected level of relic gravitational waves. This is a fundamentally important signal from the very early Universe. Its explanation requires cosmological notions and some elements of quantum physics. Since the relic gravitational waves and primordial density perturbations is presently one of the most fascinating and active areas of research, we devote to it a separate section.

V. GRAVITATIONAL WAVES AND COSMOLOGY

A. Generation of relic gravitational waves and primordial density perturbations

In many situations one can neglect the non-linearity of the gravitational field, that is, the interaction of gravitational waves with other gravitational fields and with themselves. However, this is not always the case. The most dramatic example is the interaction of gravitational waves with the strong variable gravitational field of the very early Universe. A gravitational wave can be thought of as a harmonic oscillator, while the smooth variable gravitational field of the surrounding Universe as a gravitational pump field. The g.w. oscillator is parametrically coupled to the gravitational pump field. This specific coupling is a consequence of the non-linear nature of the Einstein equations. The coupling provides a mechanism for the superadiabatic (parametric) amplification of classical waves and the quantum-mechanical generation of waves from their zero-point quantum oscillations [51]. The word “superadiabatic” emphasizes the fact that this effect takes place over and above whatever happens to the wave during very slow (adiabatic) changes of the pump field. That is, we are interested in the increase of occupation numbers, rather than in the gradual shift of energy levels. The word “parametric” emphasizes the mathematical structure of the wave equation. It is a change of a parameter of the oscillator caused by the pump field, namely, a sufficiently rapid variation of its frequency, that is responsible for the considerable increase of energy of that oscillator.

It is common to write the perturbed gravitational field of a homogeneous isotropic universe in the form:

$$ds^2 = a^2(\eta)[-d\eta^2 + (\delta_{ij} + h_{ij})dx^i dx^j]. \quad (15)$$

The gravitational field perturbations $h_{ij}(\eta, \mathbf{x})$ can be expanded over spatial Fourier harmonics $e^{\pm i\mathbf{n}\cdot\mathbf{x}}$, where \mathbf{n} is a constant (time-independent) wave-vector,

$$h_{ij}(\eta, \mathbf{x}) = \frac{\mathcal{C}}{(2\pi)^{3/2}} \int_{-\infty}^{\infty} d^3\mathbf{n} \sum_{s=1,2} \overset{s}{p}_{ij}(\mathbf{n}) \frac{1}{\sqrt{2n}} \left[\overset{s}{h}_n(\eta) e^{i\mathbf{n}\cdot\mathbf{x}} \overset{s}{c}_{\mathbf{n}} + \overset{s*}{h}_n(\eta) e^{-i\mathbf{n}\cdot\mathbf{x}} \overset{s\dagger}{c}_{\mathbf{n}} \right]. \quad (16)$$

The polarisation tensors $\overset{s}{p}_{ij}(\mathbf{n})$, $s = 1, 2$ have different forms, depending on whether the h_{ij} represent gravitational waves or density perturbations. In the case of gravitational waves, the $\overset{s}{p}_{ij}$ describe the two familiar “plus” and “cross” polarisations introduced in Sec. 2. In the case of density perturbations, the polarisation tensors are:

$${}^1p_{ij}(\mathbf{n}) = \sqrt{\frac{2}{3}}\delta_{ij}, \quad {}^2p_{ij}(\mathbf{n}) = -\sqrt{3}\frac{n_i n_j}{n^2} + \frac{1}{\sqrt{3}}\delta_{ij}. \quad (17)$$

The Einstein equations for the gravitational field perturbations h_{ij} with the polarisation tensors (17) can only be satisfied if the h_{ij} are accompanied by perturbations in the density of matter. This is why this class of perturbations is called density perturbations. The difference between ${}^s p_{ij}(\mathbf{n})$ for, respectively, gravitational waves and density perturbations is responsible for the difference in polarisation patterns of the CMB radiation, caused by these two classes of gravitational perturbations (see Sec. 5.2 below).

For a classical field h_{ij} , the quantities $\hat{c}_{\mathbf{n}}^s$, $\hat{c}_{\mathbf{n}}^{s\dagger}$ are complex numbers. For a quantized field, they are annihilation and creation operators satisfying the conditions

$$[\hat{c}_{\mathbf{n}}^{s'}, \hat{c}_{\mathbf{m}}^{s\dagger}] = \delta_{s's} \delta^3(\mathbf{n} - \mathbf{m}), \quad \hat{c}_{\mathbf{n}}^s |0\rangle = 0, \quad ,$$

where $|0\rangle$ (for each mode \mathbf{n} and s) is the initial vacuum state defined at some η_0 in the very distant past, long before the superadiabatic regime for the given mode has started. The normalization constant \mathcal{C} is determined by the requirement that initially each mode contained only the zero-point energy $\frac{1}{2}\hbar\omega$. Then, $\mathcal{C} = \sqrt{16\pi}l_{Pl}$ for gravitational waves and $\mathcal{C} = \sqrt{24\pi}l_{Pl}$ for density perturbations, where $l_{Pl} = (G\hbar/c^3)^{1/2}$ is the Planck length. Obviously, the initial vacuum amplitude, and the entire field, should vanish, if the Planck constant \hbar is formally sent to zero.

The calculation of quantum-mechanical expectation values and correlation functions provides the link between quantum mechanics and macroscopic physics. Using the representation (16) and definitions above, one finds the variance of the gravitational field perturbations:

$$\langle 0|h_{ij}(\eta, \mathbf{x})h^{ij}(\eta, \mathbf{x})|0\rangle = \frac{\mathcal{C}^2}{2\pi^2} \int_0^\infty n^2 \sum_{s=1,2} |\hat{h}_n^s(\eta)|^2 \frac{dn}{n}. \quad (18)$$

The quantity

$$h^2(n, \eta) = \frac{\mathcal{C}^2}{2\pi^2} n^2 \sum_{s=1,2} |\hat{h}_n^s(\eta)|^2 \quad (19)$$

gives the mean-square value of the metric (gravitational field) perturbations in a logarithmic interval of n and is called the (dimensionless) power spectrum. The power spectrum of metric perturbations is a quantity of great observational importance. It defines the temporal structure and amplitudes of the g.w. signal in the frequency bands of direct experimental searches. It is also crucial for calculations of anisotropy and polarisation induced in CMB by relic gravitational waves and by other gravitational field perturbations.

To find the power spectrum at any given moment of time (for instance, today or at the moment of decoupling of CMB from the rest of matter) we need to know the mode functions $\hat{h}_n^s(\eta)$ at those moments of time. In the case of gravitational waves, the mode functions $\hat{\mu}_n^s(\eta)$ (where $\hat{\mu}_n^s(\eta) \equiv a(\eta)\hat{h}_n^s(\eta)$) are governed by the equation for the parametrically disturbed oscillator [51]:

$$\hat{\mu}_n^{s''} + \hat{\mu}_n^s \left[n^2 - \frac{a''}{a} \right] = 0. \quad (20)$$

The equation describing density perturbations in the very early Universe can also be reduced to the equation very similar to Eq. (20), and the generating mechanism will work without change. As soon as the pump field (represented by the cosmological scale factor $a(\eta)$) is known, and since the initial conditions are fully determined, the mode functions $\hat{h}_n^s(\eta)$, as well as other properties of the generated fields, are unambiguously calculable. The important (and, strictly speaking, unknown) era of cosmological evolution is the stage preceding the radiation-dominated era. We call it an initial (i) era and characterize, for simplicity of calculations, by a set of power-law scale factors: $a(\eta) = l_o|\eta|^{1+\beta}$, where l_o and β are constants.

The main properties of cosmological perturbations generated as a result of superadiabatic (parametric) amplification of their zero-point quantum oscillations are as follows (for more details see [18], [52] and references there):

1. The initial vacuum state is described by a Gaussian wavefunction. As a result of quantum-mechanical Schrodinger evolution, the vacuum state transforms into a multi-particle state known as a squeezed vacuum state. The distributions of amplitudes and phases acquire strongly unequal variances. In the general expression for the gravitational field mode,

$$h_{\mathbf{n}} = A_1 \sin(n\eta + \phi_1) \cos \mathbf{n} \cdot \mathbf{x} + A_2 \sin(n\eta + \phi_2) \sin \mathbf{n} \cdot \mathbf{x},$$

the amplitudes A_1 and A_2 are drawn from a broad Gaussian distribution, whereas the phases ϕ_1 and ϕ_2 are practically fixed and equal up to $\pm\pi$. The field is a stochastic collection of standing waves and is characterised by a strongly modulated power spectrum. This complicated statistical picture of generated cosmological perturbations is often replaced in the literature by a single word: “Gaussian”.

2. The generated gravitational field perturbations act on all sorts of matter together. There is no reason why the inhomogeneities in different sorts of matter (if more than one component of matter was dynamically important in the very early Universe) should be displaced and move with respect to each other, which would constitute the so-called isocurvature, or entropy, perturbations. This is why the generated density perturbations are often called “adiabatic”.

3. The primordial spectrum (i.e. the spectrum before processing at the radiation-dominated and matter-dominated stages) as a function of the wave-number n is fully determined by the variable pump field as a function of time η . Every interval of spectrum that can be meaningfully approximated as a power-law function of n , was generated by an interval of a power-law evolution $a(\eta) \propto |\eta|^{1+\beta}$. Concretely, for the spectrum of Eq. (19) one finds: $h^2(n) \propto (l_{Pl}/l_o)^2 n^{2(\beta+2)}$. Specifically for density perturbations, one often uses the spectral index n , related to β by $n = 2\beta + 5$. If the very early Universe was governed by a scalar field (the central assumption of inflationary scenaria), then, at every power-law interval of evolution and, hence, at every power-law interval of the generated spectrum, there must be $\beta \leq -2$ and $n \leq 1$. The “red” spectra $\beta < -2$ ($n < 1$) possess a serious theoretical difficulty: the mean-square value of the field becomes power-law divergent in the limit of very long waves (lower limit of integration in Eq.(18)). The case $\beta = -2$ ($n = 1$) is called the flat, or Harrison-Zeldovich-Peebles, or “scale-invariant”, spectrum.

4. Gravitational waves are generated inevitably, whereas the generation of density perturbations requires additional assumptions about the coupling of matter fields to gravity. The primordial (unprocessed) amplitudes of density perturbations can be as large as g.w. amplitudes, but never much larger. The observed CMB anisotropy in lower multipoles (caused by primordial gravitational field perturbations) may have nothing to do with quantum mechanics, but if it does, the contribution of relic gravitational waves to lower multipoles must be substantial.

5. The parametric mechanism is universal, and the generation of primordial cosmological perturbations takes place regardless of whether the Universe 13 billion years later will appear to astronomers as spatially-flat, or not. In any case, if Ω_{total} is not identically 1, the present-day Ω_{total} is usually regulated “by hand” through the duration of the initial era. This parameter of duration does not affect seriously the amplitudes and spectral slopes of primordial perturbations.

B. Detection of relic gravitational waves

The direct detection of relic gravitational waves will be fundamentally important for uncovering the physics of the very early Universe. In Fig.6 we show the expected spectrum of today’s r.m.s. amplitudes $h(\nu)$ (square root of Eq. (19)) as a function of frequency ν in Hz . The graph shows the piece-wise envelope of the spectrum and ignores its oscillations. Almost everything in this graph is the processed spectrum; the primordial part survives only at frequencies $\nu < \nu_H$, where $\nu_H = c/\lambda_H = H \approx 2 \times 10^{-18} Hz$ is the Hubble frequency. This particular spectrum was derived under the assumption that a significant fraction of the observed large-scale CMB anisotropy is caused by relic gravitational waves and that the primordial spectral index is $\beta = -1.9$ ($n = 1.2$). This value of n follows from the COBE data [53] and it has been recently reinforced, albeit with broad error bars, by more sophisticated analysis [54]. The evaluations of n based on larger data sets usually lead to smaller n ’s, varying in a narrow interval around $n = 1$. However, this precision appears to be artificial (caused by the excessively rigid apriori assumptions about the tested models) and the story does not seem to be over. In any case, we use Fig.6 for the analysis of detectability of relic gravitational waves.

The r.m.s. values $h(\nu)$ are directly entering the detectability evaluation, but they also determine the $\Omega_{gw}(\nu)$ -parameter, which is useful for comparison of the g.w. background with other energy components. This parameter can be calculated according to the formula

$$\Omega_{gw}(\nu) = \frac{\pi^2}{3} h^2(\nu) \left(\frac{\nu}{\nu_H} \right)^2.$$

For example, one has $h(\nu) \approx 10^{-20.5}$, $\Omega(\nu) \approx 10^{-11}$ at $\nu = 10^{-3} Hz$, and $h(\nu) \approx 10^{-25}$, $\Omega(\nu) \approx 10^{-10}$ at $\nu = 10^2 Hz$. It is seen from Fig. 5 that the part of the spectrum accessible to LISA is higher than the instrumental noise and can be measured. The ground-based advanced interferometers are also promising. The target value of the LIGO-II at $\nu = 10^2 Hz$ is $h_{ex} = 10^{-23}$. The gap in two orders of magnitude can be covered by cross-correlation of the outputs of

two or more detectors. The S/N will be better than 1 if the common integration time exceeds 10^6 sec . This does not seem to be a hopeless task.

It is possible that relic gravitational waves will be first observed indirectly, with the help of polarisation measurements of CMB. The problem is to distinguish the polarisation pattern caused by gravitational waves from that caused by density perturbations. The polarisation arises as a result of the Thompson scattering of CMB photons on free electrons [55]. To produce a net polarisation, the electrons should be illuminated by CMBR having a non-zero quadrupole anisotropy. The two polarisation patterns are distinguishable if the quadrupole anisotropies are distinguishable. For our purposes of illustration, it is sufficient to consider the emission (rather than scattering) of electromagnetic waves by free electrons. The electrons are set in motion by, respectively, gravitational waves and density perturbations.

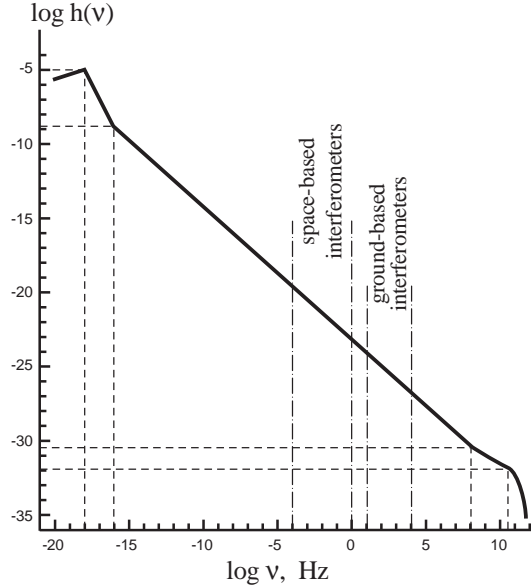


FIG. 6. Expected envelope of the spectrum $h(\nu)$ for the case $\beta = -1.9$ ($n = 1.2$)

The motion of free particles in the field of a linearly-polarised gravitational wave is shown in Fig.1. Imagine that the moving particles are free electrons in the early Universe, rather than free mirrors of an interferometer in laboratory, that we were discussing in Sec.3. Then, the directions of the induced oscillations of the electrons, indicated by arrows in Fig.1, are, at the same time, the directions of the electric fields of the electromagnetic waves emitted by these oscillating electrons. The pattern of arrows seen on this figure is the pattern of polarisation components that will be seen on the sky.

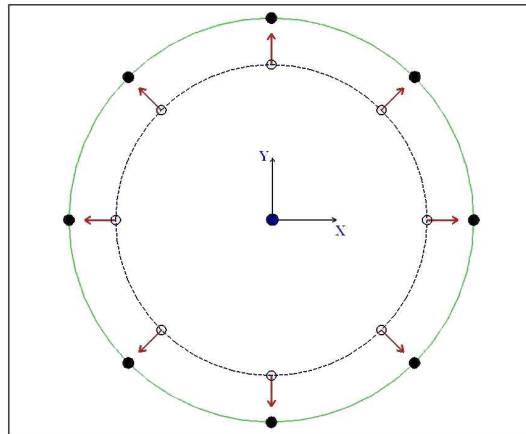


FIG. 7. Motion of free particles in the gravitational field of a density perturbation

The motion of free electrons induced by the gravitational field of a density perturbation is different. Two polarisation tensors of a density perturbation are given by Eq. (17). The first one describes a trivial purely spherically-symmetric

deformation of a sphere of free particles. The second one, subject of our interest, describes the deformation which has the angular dependence of the spherical harmonic $Y_{lm}(\theta, \phi)$ with $l = 2$ and $m = 0$, in contrast to the combination of $Y_{lm}(\theta, \phi)$ with $l = 2$ and $m = \pm 2$, attributable to a gravitational wave. In both cases, the polar axis z is taken along the wave-vector \mathbf{n} of the perturbation. Fig.7 shows a ring of electrons set in motion by the gravitational field of a density mode. The pattern of these arrows is, at the same time, the pattern of polarisation components generated by a density perturbation. Comparing Fig.1 and Fig.7 one concludes that the polarisation patterns are distinguishable, if one can study the distribution of polarisation Stokes parameters over a sufficiently large portion of the sky. In real conditions, the free electrons will be influenced by the superposition of many perturbation modes with arbitrary wave-vectors, but the net difference between these two sorts of perturbations should survive.

The gap between the expected g.w. signal and the polarisation detection capabilities is relatively small. Taking into account the current impressive activity in this area, one can hope that some decisive observational information about relic gravitational waves can be obtained pretty soon.

C. Gravitational waves and inflation

The theoretical and experimental studies of relic gravitational waves are endangered by absurd claims that are prevalent in inflationary literature. Inflationists claim that the amount of relic gravitational waves should be zero if the primordial spectrum is flat, that is, if $n = 1$. There seems to be no need to bother about relic gravitational waves, as the observations indicate that n may indeed be close to 1. Since the “pillars of inflation” are popular in a part of astrophysics community, and sometimes are said to be “confirmed”, it is important to put matters straight.

Inflationary scenario operates with a scalar field φ and the scalar field potential $V(\varphi)$. Having accepted the general concept of parametrically amplified quantum fluctuations, inflationary theorists are performing their own calculations. The quantum-mechanical content of these calculations is usually limited to vague words, such as that “inflation amplified quantum fluctuations onto macroscopic scales”. Being unsure why and where the Planck constant \hbar should enter the calculations, inflationists never write it explicitly; and when it is written implicitly, in the form of the Planck mass, $M_{Pl} = (\hbar c/G)^{1/2}$, it always stands in the wrong place, in the denominator of the final expression instead of the nominator. With this sort of “quantisation”, inflationary theorists derived their contribution to the subject of cosmological perturbations – the “standard inflationary result”. The “standard inflationary result” predicts the infinitely large amplitudes of today’s density perturbations in the limit of the flat spectrum $n = 1$. Indeed, one will always be able to recognise in inflationary papers the evaluations relating the final (f) amplitudes of the perturbations to the initial (i) values of φ and other quantities: $(\delta\rho/\rho)_f \sim (h_S)_f \sim (\zeta)_f \approx (\zeta)_i \sim (H^2/\dot{\varphi})_i \sim (V^{3/2}(\varphi)/V'(\varphi))_i \sim H_i/\sqrt{1-n}$. The denominator of the last expression is zero for $n = 1$. The nominator is the Hubble parameter H_i at the initial stage. H_i is much larger than the Hubble parameter at the subsequent radiation-dominated stage, and, in any case, H_i is not zero. Therefore, the predicted final amplitudes go to infinity, if the spectral index $n = 1$. Inflationists are hiding this absurd prediction of infinitely large density perturbations by composing the ratio of the gravitational wave amplitude h_T to the predicted divergent amplitude of the scalar metric perturbations h_S (the so called “tensor-to-scalar ratio” or “consistency relation”: $h_T/h_S \approx \sqrt{1-n}$) and declaring that it is the amount of gravitational waves that should be zero, or almost zero, at cosmological scales and, hence, down to laboratory scales.

Certainly, the “standard inflationary result” is in full disagreement not only with the theoretical quantum mechanics, but with available observations too, as long as the error-boxes of the observationally derived spectral index n are centered at $n \approx 1$ and include $n = 1$. To be consistent with inflationary predictions, the data should not allow “blue” spectra $n > 1$, as the scalar field cannot produce them, and the density amplitudes should go to infinity, when one processes the data assuming that $n = 1$. This spectacular failure of inflationary calculations is systematically painted by inflationists and their followers as a great success. The most recent example is the analysis of WMAP data [56]. The authors praise and follow inflationary derivations, and conclude that the “tensor/scalar ratio r ” is “consistent with zero”. The “standard inflationary result” is written in that paper (their formula (17)) as:

$$\Delta_{\mathcal{R}}^2 = \frac{V/M_{Pl}^4}{24\pi^2\epsilon_V},$$

and the “tensor/scalar ratio r ” (their formula (18)) as:

$$r = 16\epsilon_V.$$

Combining the second formula with the first one, one can easily see that if the WMAP data demonstrate that “ r is consistent with zero”, then the WMAP data should also be consistent with an infinite numerical value of the density amplitudes $\Delta_{\mathcal{R}}^2$ and, hence, with an infinite numerical value of the induced CMB anisotropies. If the WMAP data are

not consistent with such an infinite numerical value of density perturbations, then the only “implication for inflation” that follows from the WMAP observations is that the single concrete formula derived by inflationists – their “standard inflationary result” – is shown to be wrong.

It seems to the author that overenthusiasm for inflation has reached unscientific, even ecclesiastical proportions. For example, this is how inflation is characterized in the educational program “Astronomy” of the Smithsonian Institutions [57]: “...the inflationary scenario is the best current theory of the Universe...It has met four critical observational tests...”. It is unclear which 4 tests the inflationary school credits to itself, rather than to direct consequences of quantum mechanics and general relativity, but one can recall that even general relativity was characterized until quite recently as a theory that has met only 3 critical observational tests (1 of which, gravitational red-shift, is not a test of specifically general relativity). As for professional papers, one reads almost every day claims that the CMB and galaxy surveys are “in spectacular agreement with an inflationary Λ -dominated cold dark matter cosmology” (compare, for example, with [58] and [59]). Somewhere in the text, authors usually admit that, say, the observed quadrupole anisotropy is way out of the predicted value, and that the probability of finding such a result within the “standard” model is 1.5×10^{-3} [60], [58]. Surely a theory which is admitted to have only a one on a thousand chance of being consistent with one of its crucial observational tests is not in “spectacular agreement” with the cosmos we are trying to understand and should not be a subject given to self-congratulation.

D. Gravitational waves and quadrupole anisotropy

The accurate measurements of CMB by WMAP reiterate the issue of the gravitational wave contribution to the lower order multipoles. The best strategy is to rely on conclusions of general physics and to use the minimum number of extra hypotheses. If the general considerations suggest (see Sec.5.1) that the contributions of gravitational waves and density perturbations should be of the same order of magnitude, it is this conclusion that should be tested most thoroughly.

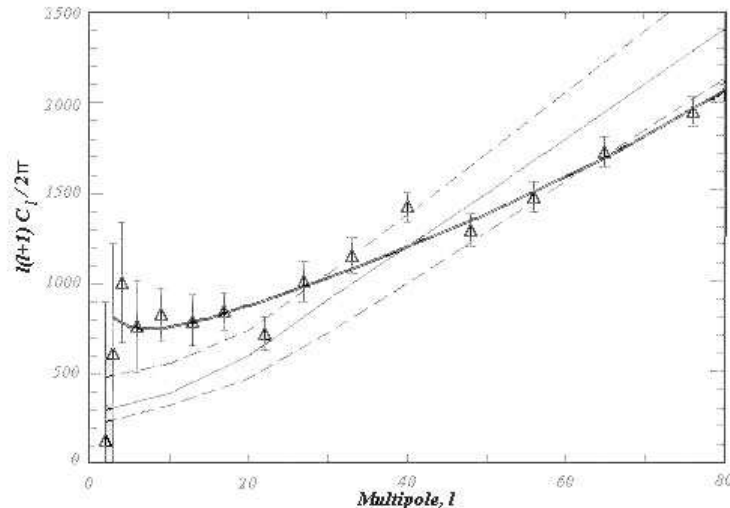


FIG. 8. The WMAP data and some theoretical models

Fig.8 shows [61] the WMAP observational points (triangles) and the best fit curve (solid line) of the Λ -dominated cosmology without gravitational waves. The predicted quadrupole ($l = 2$) anisotropy is a factor of 8 higher than the actually observed value. The thin solid line (reproduced from [52], fig.12) shows the contribution of density perturbations alone in a model with $z_{dec} = 1000$, $z_{eq} = 5000$, $n = 1$ that fits the position and value of the peak at $l = 220$. This line is surrounded by the 1σ uncertainty belt (shown by two dashed lines) arising due to the lack of ergodicity on a 2-sphere. At sufficiently large l 's the belt is approximately symmetric and its size is $\Delta C_l \approx \sqrt{2/(2l+1)}C_l$. But the asymmetry grows towards small l 's, and specifically at $l = 2$ the size of the deviation down is only 0.4 part of the deviation up [62]. [The accurate displaying of this fundamental uncertainty makes the actual quadrupole even further out of the uncertainty belt of the Λ -dominated cosmology, than what is implied by the usually plotted symmetric “cosmic variance”.] Comparing the thin line with the data points, it is difficult to avoid the conclusion (advocated in [52]) that in fact there exists an excess, rather than a deficit, of power at small multipoles, and the most natural

explanation of this excess is the anticipated contribution of gravitational waves. The increase of the spectral index up to $n = 1.2$ makes the agreement with the observed quadrupole even better and implies a somewhat larger amount of gravitational waves [52]. One should remember, however, that all the experimental C_l data, together with all the cosmological parameters, is a finite set of numbers. At the same time, in our hands is the (strictly speaking, unknown) shape of the primordial spectrum, i.e. a continuous function and an infinite set of numbers. A perfect agreement with any observed C_l 's and practically any set of cosmological parameters, not only $\Lambda = 0$, can be achieved at the expense of the properly chosen primordial spectrum. Unfortunately, the era of “precision cosmology” is still at some distance from us.

The nature of the observed quadrupole anisotropy deserves special attention. Most likely, it is caused by superposition of very long gravitational and density waves. It is known [63] that a gravitational wave produces the $Y_{2,2}$ and $Y_{2,-2}$ CMB anisotropy, whereas a density perturbation produces the $Y_{2,0}$ CMB anisotropy. We have discussed this distinction in Sec.5.2 in connection with the CMB polarisation. The actual quadrupole distribution over the sky was measured by COBE [64]. In Galactic coordinates,

$$Q(\theta, \phi) = Q_1(3 \cos^2 \theta - 1)/2 + Q_2 \sin 2\theta \cos \phi + Q_3 \sin 2\theta \sin \phi + Q_4 \sin^2 \theta \cos 2\phi + Q_5 \sin^2 \theta \sin 2\phi,$$

where the measured (least noisy) components are [65]:

$$Q_1 = 19.0 \pm 7.4, \quad Q_2 = 2.1 \pm 2.5, \quad Q_3 = 8.9 \pm 2.0, \quad Q_4 = -10.4 \pm 8.0, \quad Q_5 = 11.7 \pm 7.3. \quad (21)$$

Even if this $Q(\theta, \phi)$ is produced by a single gravitational wave or a single density perturbation, it is only in a special coordinate system that it can be reduced to the combination of $Y_{2,2}$ and $Y_{2,-2}$ or to $Y_{2,0}$, respectively. To find out what we are dealing with, we have to build invariants, that is, quantities independent of the rotation of the coordinate system. One of invariants is

$$Q_{rms}^2 = (4/15)[(3/4)Q_1^2 + Q_2^2 + Q_3^2 + Q_4^2 + Q_5^2],$$

another one (see, for example, [66]) is

$$D = (4/5^{3/2})[(1/4)Q_1(Q_1^2 + Q_2^2/2 + Q_3^2/2 - Q_4^2 - Q_5^2) + 2Q_2Q_3Q_5 + Q_4(Q_2^2 - Q_3^2)].$$

Q_{rms} is always positive, whereas D can be negative, but it always satisfies the condition $|D| \leq Q_{rms}^3$. For a pure density perturbation, $|D| = Q_{rms}^3$; and for a pure gravitational wave, $D = 0$.

Calculating the invariants and the formal errors from the data set (21) we find

$$Q_{rms} = (12.6 \pm 3.4)\mu K, \quad -D^{1/3} = (6.9 \pm 12.9)\mu K$$

As expected, the available noisy data do not allow one to prefer one of hypotheses over another. But, for sure, there is no indications whatsoever that the quadrupole anisotropy is produced by a density perturbation alone. If anything, the central values of Q_{rms} and D indicate that the contribution of gravitational waves should be substantial. Hopefully, the WMAP quadrupole data will be more accurate, and then this analysis should be repeated.

VI. SUMMARY

Gravitational-wave physics is a mature and at the same time a very young science. In a sense, the relativistic gravity (general relativity) itself is still a young science. The enormous progress in technical developments and observational verifications of the theory is accompanied by difficult issues of its adequate description and interpretation, the necessity of bringing it to a closer contact with other branches of physics.

It is rumored that the Nobel recognition eluded the great astronomer E. Hubble because of his reluctance to say about his discovery what the establishment wanted him to say. Apparently, the scientific integrity of E. Hubble allowed him to say what he believed he discovered – the nonstationarity of the system of nearby galaxies – whereas he was required to admit that he discovered the “expansion of space”. But the “expansion of space” is still alive and well. [For example, “As bizarre as it may seem, space itself is expanding – specifically, the vast regions of space between galaxies” [57].] It is regularly proposed to be measured. The logic seems to be impeccable. If “space” expands by a factor of 2 in 10 billion years, why would not the Earth or an atom expand by 10% in 1 billion years? The gravitational-wave research is plagued in a similar fashion. It is often stated that “gravitational waves are oscillations of space-time itself”. The next phrase seems to be logically unavoidable: “gravitational waves act tidally, stretching and squeezing any object that they pass through”. If this phrase were correct, we would never be able to notice

gravitational waves. The device measuring, say, the displacements of free mirrors in an interferometer would be “stretched and squeezed” as well. In this situation, we can probably find comfort in the wise observation [67]: “I agree that much of what one reads in the literature is absurd. Often it is a result of bad writing, rather than bad physics. I often find that people who say silly things actually do correct calculations, but are careless in what they say about them.”

It seems to the author that, in the long perspective, the value of the gravitational wave research will be in its influence on the fundamental physics. Meanwhile, let us hope that the next gravitational-wave update will be devoted to the fascinating nature of concrete astrophysical sources of gravitational waves detected by the existing instruments.

ACKNOWLEDGMENTS

I am grateful to S.Babak, D.Baskaran, and B.Sathyaprakash for help and useful discussions.

-
- [1] A. Einstein. Zum gegenwertigen Stande des Gravitationsproblems, *Phys. Z.* **XIV**, 1249-1266 (1913)
 - [2] J. Weber. *Phys. Rev.* **117**, 306 (1960); *General Relativity and Gravitational Waves*, (New York: Interscience Publ. 1961)
 - [3] J. H. Taylor. *Rev. Mod. Phys.* **66**, 711 (1994)
 - [4] <http://igec.lnl.infn.it>
 - [5] <http://www.ligo.org>
 - [6] <http://www.ligo.caltech.edu>
 - [7] <http://www.geo600.uni-hannover.de>
 - [8] <http://www.virgo.infn.it>
 - [9] <http://tamajo.mtk.nao.ac.jp>
 - [10] P. Astone *et al.*, arXiv:astro-ph/0302482
 - [11] <http://www.lisa.jpl.nasa.gov>
 - [12] L. D. Landau and E. M. Lifshitz. *Classical Theory of Fields*, (Oxford: Pergamon Press, 1975)
 - [13] C. W. Misner, K. S. Thorne and J. A. Wheeler. *Gravitation*, (San Francisco: W.H.Freeman and Co., 1975)
 - [14] S. Weinberg. *Gravitation and Cosmology*, (New York: J. Wiley and Sons, 1972)
 - [15] K. S. Thorne. In *Three Hundred Years of Gravitation*, Eds. S. W. Hawking and W. Israel, (Cambridge:CUP, 1987) p. 330
 - [16] L. P. Grishchuk. *Usp. Fiz. Nauk* **121**, 629 (1977) [*Sov. Phys. Usp.* **20**, 319 (1977)]
 - [17] B. F. Schutz. *Class. Quant. Grav.* **16**, A131 (1999)
 - [18] L. P. Grishchuk, V. M. Lipunov, K. A. Postnov, M. E. Prokhorov and B. S. Sathyaprakash. *Usp. Fiz. Nauk* **171**, 3 (2001) [*Physics-Uspekhi* **44**, 1 (2001); arXiv: astro-ph/0008481]
 - [19] C. Cutler and K. S. Thorne. In: *General Relativity and Gravitation*, Eds. N.T.Bishop and S.D.Maharaj, (World Scientific, 2002) p. 72
 - [20] D. Baskaran and L. P. Grishchuk. *in preparation*
 - [21] <http://www.minigrail.nl>; E. Coccia *et al.* *Phys. Rev. D* **57**, 2051 (1998)
 - [22] P. Astone *et al.* *Class. Quant. Grav.* **19**, 5449 (2002)
 - [23] L. S. Finn. arXiv: gr-qc/0301092
 - [24] P. Astone *et al.* arXiv: gr-qc/0304004
 - [25] L. Blanchet. In: *General Relativity and Gravitation*, Eds. N.T.Bishop and S.D.Maharaj, (World Scientific, 2002) p. 54
 - [26] B. Barish. AAAS meeting, <http://php.aaas.org/meetings>
 - [27] T. A. Prince, M. Tinto, S. L. Larson, and J. W. Armstrong. *Phys. Rev. D* **66**, 122002 (2002)
 - [28] N. J. Cornish and S. L. Larson. arXiv: astro-ph/0301548
 - [29] A. Krolak and M. Tinto. arXiv: astro-ph/0302013
 - [30] E. S. Phinney. *Astroph. J. Lett.* **380**, L17 (1991)
 - [31] V. M. Lipunov, K. A. Postnov and M. E. Prokhorov. *Pis'ma Astron. Zh.* **23**, 563 (1997) [*Astron. Lett.* **23**, 492 (1997)]
 - [32] V. Kalogera, R. Narayan, D. N. Spergel, and J. H. Taylor. *Astroph. J.* **556**, 340 (2001)
 - [33] C. Kim, V. Kalogera, and D. R. Lorimer. arXiv: astro-ph/0207408
 - [34] M. S. Sipior and S. Sigurdsson. *Astroph. J.* **572**, 962 (2002)
 - [35] F. A. Rasio. arXiv: astro-ph/0212211
 - [36] S. Sigurdsson. *Black Holes and Pulsar Binaries*, arXiv: astro-ph/0303312
 - [37] E. E. Flanagan and S. A. Hughes. *Phys. Rev. D* **57**, 4535 (1998)
 - [38] A. Buonanno and T. Damour. *Phys. Rev. D* **62**, 064015 (2000)

- [39] L. Lehner. *Class. Quant. Grav.***18**, R25 (2001)
- [40] M. Rees, R. Ruffini, and J. A. Wheeler. In: *Black Holes, Gravitational Waves, and Cosmology* (Gordon and Breach, New York, 1974)
- [41] D. M. Eardley. In: *Gravitational Radiation*, eds. N. Deruelle and T. Piran (North Holland, Amsterdam, 1983) p.257
- [42] K. C. B. New. *Gravitational Waves from Gravitational Collapse*, arXiv: gr-qc/0206041
- [43] N. Andersson. *Gravitational waves from instabilities in relativistic stars*, arXiv: astro-ph/0211057
- [44] M. A. Papa, B. F. Schutz, and A. M. Sintes. arXiv: gr-qc/0011034
- [45] P. R. Brady, T. Creighton, C. Cutler, and B. F. Schutz. *Phys. Rev. D***57**, 2101 (1998)
- [46] C. Cutler and A. Vecchio. In: *Proceedings of the 2nd LISA Symposium*, ed. W.M.Folkner, (Am. Inst. Phys., 1998) p.95
- [47] S. Shapiro. arXiv: astro-ph/0304202
- [48] A. Vecchio. *LISA observations of rapidly spinning massive black hole binary systems*, arXiv: astro-ph/0304051
- [49] G. Kauffmann and M. G. Haehnelt. *MNRAS* **311**, 576 (2000)
- [50] B. S. Sathyaprakash and B. F. Schutz. *Templates for stellar mass black holes falling into supermassive black holes*, arXiv: gr-qc/0301049
- [51] L. P. Grishchuk. *Zh. Eks. Teor. Fiz.* **67**, 825 (1974) [*Sov. Phys. JETP* **40**, 409 (1975)]; *Ann. NY Acad. Sci.* **302**, 439 (1977)
- [52] D. Dimitropoulos and L. P. Grishchuk. *Int. J. Mod. Phys. D***11**, 259 (2002); S. Bose and L. P. Grishchuk. *Phys. Rev. D* **66**, 043529 (2002); L. P. Grishchuk. In: *2001: A Relativistic Spacetime Odyssey*, Eds. I.Ciufolini, D. Dominici, L. Lusanna. (World Scientific, 2003) p. 223 [arXiv:gr-qc/0202072]
- [53] G. F. Smoot *et al.* *Astroph. J. Lett.* **396**, L1 (1992); C. L. Bennet *et al.* *Astroph. J. Lett.* **464**, L1 (1996); K. M. Gorski *et al.* *Astroph. J.* **464**, L1 (1996).
- [54] D. Maino, A. J. Banday, C. Baccigalupi, F. Perrotta, K. M. Gorski. *Astrophysical components separation of COBE-DMR 4yr data with FastICA*, arXiv:astro-ph/0303657
- [55] M. J. Rees. *Astroph. J.* **153**, L1 (1968); A. G. Polnarev. *Sov. Astron.* **29**, 607 (1985); M. Zaldarriaga and U. Seljak. *Phys. Rev. D.* **55**, 1830 (1997); M. Kamionkowski, A. Kosowsky, and A. Stebbins. *Phys. Rev. D.* **55**, 7368 (1997)
- [56] H. V. Peiris *et al.* *First year WMAP observations: implications for inflation*, arXiv:astro-ph/0302225
- [57] <http://www.si.edu/scienceandtechnology/astronomy>
- [58] G. Efstathiou. *Is the low CMB quadrupole a signature of spatial curvature ?*, arXiv:astro-ph/0303127
- [59] S. L. Bridle, O. Lahav, J. P. Ostriker, and P. J. Steinhardt. *Precision cosmology ? Not just yet...*, arXiv:astro-ph/0303180
- [60] D. N. Spergel *et al.* *First year WMAP observations: determination of cosmological parameters*, arXiv:astro-ph/0302207
- [61] I am grateful to P. Mauskopf and D. Baskaran for composing Fig. 8.
- [62] L. P. Grishchuk *Phys. Rev. D***53**, 6784 (1996); L. P. Grishchuk and J. Martin *Phys. Rev. D***56**, 1924 (1997)
- [63] L. P. Grishchuk and Ya. B. Zeldovich. *Astron. Zhurn.***55**, 209 (1978) [*Sov. Astron.* **22**, 125 (1978)]
- [64] A. Kogut, G. Hinshaw, A. J. Banday, C. L. Bennet, K. Gorski, G. F. Smoot, and E. L. Wright. arXiv astro-ph/9601060
- [65] I am grateful to G. Smoot for the clarifying correspondence.
- [66] J. C. R. Magueijo. *Cosmic confusion*, arXiv: astro-ph/9412096
- [67] I am grateful to S. Weinberg for the permission to quote his e-mail message of 25 Feb 2003